

Nucleophilic Addition to Olefins. 15.¹ Solvent and Substituent Effects on the Hydrolysis of Benzylidenemalononitriles in Basic Me₂SO-Water Solutions

Claude F. Bernasconi,* John P. Fox, Anastassia Kanavarioti, and Markandeswar Panda

Contribution from the Thimann Laboratories of the University of California, Santa Cruz, California 95064. Received August 26, 1985

Abstract: Benzylidenemalononitriles hydrolyze to ArCHO and CH(CN)₂⁻ in basic solution. A kinetic study of this reaction with the parent compound and with the 4-NMe₂, 4-OMe, 3-Cl, 4-CN, and 4-NO₂ derivatives in water and in 30%, 50%, 60%, and 70% aqueous Me₂SO is reported. In water nucleophilic addition of OH⁻ to the olefin (*k*₁^{OH}, Scheme I), to form ArCH(OH)C(CN)₂⁻ (T_{OH}⁻) is rate limiting with all substrates. In the Me₂SO-containing solvents, the formation of T_{OH}⁻ at high [KOH] becomes faster than its conversion to products. This allows separate measurement of the rate of product formation. The major pathways for this latter process involve rate-limiting intramolecular proton switch (*k*₁, Scheme II) and rate-limiting carbon protonation of the dianionic intermediate ArCH(O⁻)C(CN)₂⁻ (T_O²⁻) by water (*k*₆^{H₂O}, Scheme II); the most "obvious" pathway through rate-limiting carbon protonation of T_{OH}⁻ by water (*k*₂^{H₂O}) is insignificant, but carbon protonation of T_{OH}⁻ by piperidinium ion (*k*₂^{BH}) is important. At very high base concentration, there is a further change to rate-limiting breakdown of ArCH(O⁻)CH(CN)₂ (T_O⁻) (*k*₄) for the 3-Cl and 4-NO₂ derivatives but not for the other substrates. The intramolecular proton switch (*k*₁) is best understood as a concerted proton transfer with a transition state that includes a water bridge. Two kinetically equivalent alternatives involve carbon protonation of T_O²⁻ by H₃O⁺, with transition stabilization by hydrogen bonding between H₃O⁺ and O⁻, and carbon protonation T_{OH}⁻ by water, with transition-state stabilization by hydrogen bonding between the hydroxy group of T_{OH}⁻ and the incipient hydroxide ion. Both alternatives can be excluded because they cannot account for the high *k*₁ values. On the basis of the substituent and solvent effects on the rate (*k*₁^{OH}) and equilibrium constants (*K*₁^{OH}) of OH⁻ addition, the following conclusions are drawn: (1) There is an imbalance between the polar substituent effect (*ρ*_{nor}) and the response of *k*₁^{OH} to the decreased solvation of OH⁻ in the Me₂SO-containing solvents (*β*_{nuc,sol}). This may be attributed to a combination of factors, such as a lag in the resonance stabilization of the C(CN)₂⁻ moiety in T_{OH}⁻, an early desolvation of the OH⁻ ion, and an electrostatic interaction in the transition state between the residual negative charge on the attacking OH⁻ and the aryl substituent. (2) The *ρ*(*k*₁^{OH}) values depend very little on solvent, and the solvent effect on *k*₁^{OH} (*β*_{nuc,sol}) depends very little on the aryl substituent. This indicates that the cross-correlation coefficient *ρ*_{xs} = ∂*ρ*(*k*₁^{OH})/∂ log *γ*_{OH⁻} = ∂*β*_{nuc,sol}/∂*σ* ≈ 0, with *γ*_{OH⁻} being the solvent activity coefficient for the transfer of OH⁻ from water to Me₂SO-water mixtures.

The mechanism of hydrolysis of benzylidenemalononitrile (BMN) involves a series of steps as shown in Scheme I. We have recently embarked on a detailed study of this reaction. Part of our findings have been published in two recent papers.² In the first paper, we reported our results in acidic and basic aqueous solution,^{2a} while the second dealt with the reaction in acidic Me₂SO-water solutions.^{2b} The major conclusions from these two papers can be summarized as follows:

(1) In aqueous solution, none of the intermediates accumulate to detectable levels, and the following steps are rate-limiting: *k*₁^{OH} at pH ≥ 8.0; *k*₁^{H₂O} at pH 5.0-8.0; *k*₄ at pH 0.3-5.0; *k*₃₄^{H₂O} at pH ≤ 0.3. We were able to measure *k*₁^{OH} and *k*₁^{H₂O} directly and to estimate all the other rate constants shown in the scheme.

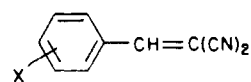
(2) As Me₂SO is added to the solvent, the T_O⁻ adduct is destabilized which leads to an increase in the rate constant of its breakdown into benzaldehyde and CH(CN)₂⁻ (*k*₄ step). As a consequence, there is a change from *k*₄ << *k*₋₃^{H₂O}*a*_{H+} + *k*₋₃^{H₂O} + *k*₋₃^{BH}[BH] to *k*₄ > *k*₋₃^{H₂O}*a*_{H+} + *k*₋₃^{H₂O} + *k*₋₃^{BH}[BH], and deprotonation of T_{OH}⁰ becomes partially rate limiting in moderately acidic solution. This manifests itself by the observation of general base catalysis.

(3) Even in water, the *k*₄ step is remarkably fast (~5 × 10⁴ s⁻¹ at 25 °C, ~3.3 × 10⁴ s⁻¹ at 20 °C) considering the relatively high basicity of CH(CN)₂⁻ (p*K*_a^{CH₂(CN)₂} = 11.19 at 25 °C, 11.39 at 20 °C). This indicates that the nucleofugality of CH(CN)₂⁻ in carbonyl-forming elimination reactions is about as high as that of oxyanions or amines of the same basicity.

(4) The estimated intrinsic rate constant,³ *k*₀, for the *k*₄ step is much greater than for the breakdown of the corresponding T_O⁻ adduct derived from a *β*-nitrostyrene. The same kinetic advantage of the dicyano over the nitro compound is also found in the addition of hydroxide ion to the C=C double bond (*k*₁^{OH}). These findings are consistent with a generally observed pattern of lower intrinsic

rates (higher intrinsic barriers) in the formation of more strongly resonance-stabilized carbanions.⁴

In the present paper, we examine the effect of adding Me₂SO and of varying the substituent in the phenyl group of BMN on the reaction in basic solution. This is the pH range where the nucleophilic addition steps (*k*₁^{H₂O} and *k*₁^{OH}) are rate-limiting for the parent compound in aqueous solution. The substrates studied are



- X • 4-NO₂ (BMN-NO₂)
- X • 4-CN (BMN-CN)
- X • 3-Cl (BMN-Cl)
- X • H (BMN)
- X • 4-OMe (BMN-OMe)
- X • 4-NMe₂ (BMN-NMe₂)

Results

Products. Hydrolysis products were identified by their UV spectra. In water both the absorption of the respective benzaldehydes (*λ*_{max} = 265, 250, 246, 247, 282, and 351 nm for X = 4-NO₂, 4-CN, 3-Cl, H, 4-OMe, and 4-Me₂N, respectively) and that of CH(CN)₂⁻ (*λ*_{max} = 233 nm) are visible. In the Me₂SO-water mixtures, the spectral range <250 nm was inaccessible, and thus product formation was monitored by observing the spectra of the respective benzaldehyde only, with just a small contribution by the tail end of the CH(CN)₂⁻ spectrum.

The product solutions were not very stable and showed gradual changes in their spectrum. These changes occurred both in actual "infinity solutions" from kinetic runs and in "mock infinity solutions", prepared by mixing the respective benzaldehyde with malononitrile under the same reaction conditions. Control experiments with only malononitrile clearly showed that the changes are due to the decomposition of this latter product.

There are probably two concurrent decomposition modes:

(1) Part 14: Bernasconi, C. F.; Laibelman, A.; Zitomer, J. L. *J. Am. Chem. Soc.* **1985**, *107*, 6570.

(2) (a) Bernasconi, C. F.; Howard, K. A.; Kanavarioti, A. *J. Am. Chem. Soc.* **1984**, *106*, 6827. (b) Bernasconi, C. F.; Kanavarioti, A.; Killion, R. B. *J. Am. Chem. Soc.* **1985**, *107*, 3612.

(3) Defined for any reaction as *k* when *K* = 1.

(4) For a recent review, see: Bernasconi, C. F. *Pure Appl. Chem.* **1982**, *54*, 2335.

Scheme I

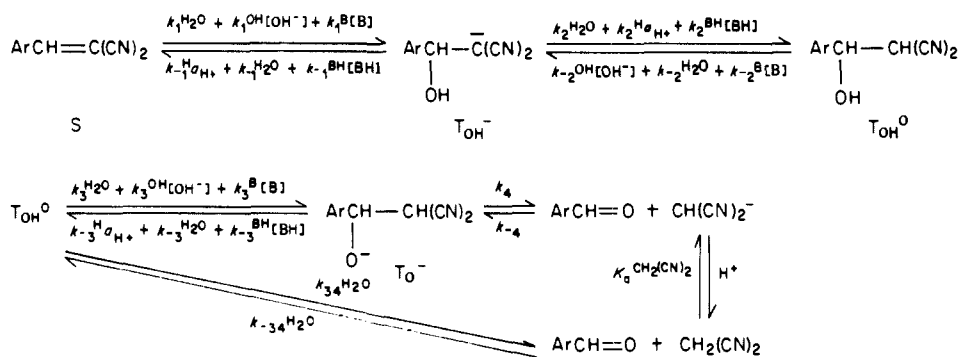


Table I. Spectral Data of Phenyl-Substituted Benzylidenemalononitriles

substituent	water		50% Me ₂ SO		60% Me ₂ SO	
	λ _{max}	log ε	λ _{max}	log ε	λ _{max}	log ε
4-NO ₂	307	4.33	308	4.32	308	4.28
4-CN						
3-Cl	300	4.26	300	4.24	300	4.24
H	308	4.33	308	4.31	309	4.32
4-OMe	350	4.45	351	4.44	351	4.43
4-NMe ₂			442	4.72		

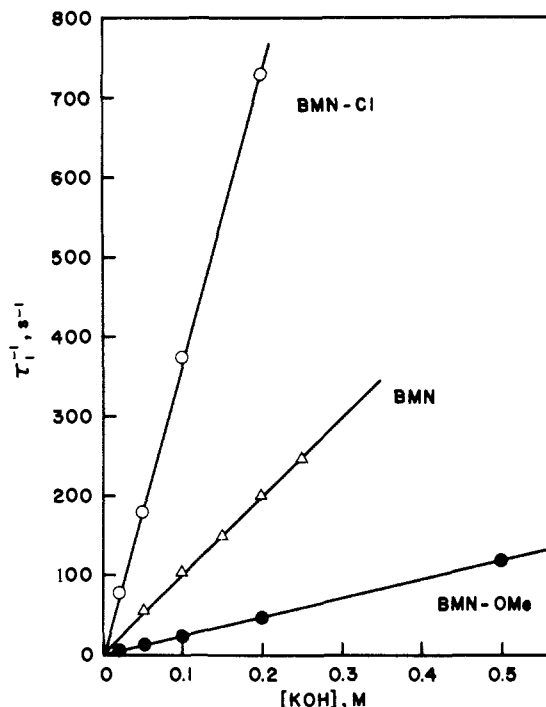
hydrolysis of one of the cyano groups and the condensation of malononitrile anion with a molecule of malononitrile.⁵ This notion is supported by the observation that in the Me₂SO richest solvents (60% and 70% Me₂SO), the spectra of the real infinity solutions differed slightly from those of the mock solutions. In these solvents, the malononitrile decomposition is quite fast and occurs already before the hydrolysis of BMN is complete. This disfavors the condensation reaction because the concentration of malononitrile/malononitrile anion cannot reach the level which prevails initially in the mock infinity solution.

Kinetics Experiments. General Features. The rates were measured in water and in 30%, 50%, 60%, and 70% aqueous Me₂SO (by volume) at 20 °C. All kinetic runs were conducted under pseudo-first-order conditions either in buffered solutions or mostly in dilute KOH. The ionic strength was maintained at μ = 0.5 M with KCl, except in 70% Me₂SO where it was 0.25 M because of reduced solubility.

Some of the problems reported before,² in particular the non-linearity of first-order kinetic plots under certain experimental conditions, were again observed. Just as before, they can be traced to the reversibility of the reaction at pH < pK_a^{CH₂(CN)₂}, and to the reaction of CH(CN)₂⁻ with unreacted substrate at pH > pK_a^{CH₂(CN)₂}, as discussed in detail in a previous report.^{2a} At high pH (usually at [OH⁻] ≥ 10⁻⁴ M), excellent first-order behavior was restored when the reaction was monitored at or near λ_{max} of the olefin (Table I). In this pH range, the observed pseudo-first-order rate constants, τ₁⁻¹, are proportional to [OH⁻], indicating that the observed process is addition of OH⁻ to the olefin as in aqueous solution.^{2a}

In the Me₂SO-containing solvents, a second, slower kinetic process was observed at high base concentrations. Its rate could be monitored in the range of 250–280 nm although the OD changes were generally not very large (ΔOD ≈ 0.1–0.2 in most cases). The spectra of the final products were the same as at lower base concentrations where only one kinetic process was observed.

This behavior is reminiscent of observations made while studying the hydrolysis of benzylidene Meldrum's acid⁶ and of 1,1-dinitro-2,2-diphenylethylene.⁷ It indicates that formation of the adduct T_{OH}⁻ (Scheme I) becomes faster than its conversion to products. The pseudo-first-order rate constant for this second process which leads to products will be called τ₂⁻¹.

Figure 1. τ₁⁻¹ as a function of [KOH] for BMN-Cl, BMN, and BMN-OMe in 50% Me₂SO–50% water at 20 °C.

τ₂⁻¹ tends to become slower with increasing Me₂SO content of the solvent and with greater electron-withdrawing strength of the phenyl substituent. These trends are opposite to those for τ₁⁻¹. Hence, the separation between τ₁⁻¹ and τ₂⁻¹ and with it the measurability of τ₂⁻¹ became better in the Me₂SO-rich solvents and for substrates with electron-withdrawing groups. For example, in 50% Me₂SO, the slow process is barely detectable with BMN-OMe at 0.5 M KOH but still well separated from the fast process with BMN-NO₂ at [KOH] = 0.02 M (τ₁⁻¹ = 374 s⁻¹, τ₂⁻¹ = 14.0 s⁻¹). On the other hand, in 70% Me₂SO, there is good separation with BMN-OMe even at [KOH] as low as 0.1 M (τ₁⁻¹ = 135 s⁻¹, τ₂⁻¹ = 9.75 s⁻¹).

Kinetics of OH⁻ Addition. Typically rates were measured at five different KOH concentrations, spanning a range of 25-fold, for each compound and each solvent mixture. The raw data are summarized in Tables S1–S5 (113 τ₁⁻¹ values) in the supplementary materials.⁸ Figure 1 shows representative plots of τ₁⁻¹ vs. [KOH] in 50% Me₂SO–water. Similar plots, indicating a rate law given by eq 1 were found in all solvents. Table II lists all the measured k₁^{OH} values in five different solvents.

$$\tau_1^{-1} = k_1^{\text{OH}}[\text{OH}^-] \quad (1)$$

Kinetics of Water and OH⁻ Addition in Buffered Solutions. A number of experiments aimed mainly at measuring the rate constant k₁^{H₂O} for water addition to BMN in 50% Me₂SO were performed. To this end, τ₁⁻¹ was measured in dilute cacodylate,

(8) See paragraph concerning supplementary material at the end of this paper.

(5) Schaeffer, F. C. In *Chemistry of the Cyano Group*; Rappoport, Z., Ed.; Wiley-Interscience: New York, 1970; p 239.

(6) (a) Bernasconi, C. F.; Leonaruzzi, G. D. *J. Am. Chem. Soc.* **1980**, *102*, 1361; (b) **1982**, *104*, 5133, 5143.

(7) Bernasconi, C. F.; Carré, D. J.; Kanavarioti, A. *J. Am. Chem. Soc.* **1981**, *103*, 4850.

Table II. Rate Constants, k_1^{OH} , for OH^- Addition to Substituted Benzylidenemalononitriles in Various Solvents at 20 °C^a

	water	Me_2SO			
		30%	50%	60%	70%
4- NO_2	1.51×10^3	5.15×10^3	1.85×10^4	3.75×10^4	1.08×10^5
4-CN			1.02×10^4		
3-Cl	3.19×10^2	1.36×10^2	3.63×10^3	7.76×10^3	2.54×10^4
H	1.26×10^2	5.20×10^2	1.00×10^3	2.30×10^3	6.75×10^3
4-OMe	2.11×10^1	9.52×10^1	2.35×10^2	5.00×10^2	1.44×10^3
4-NMe ₂			6.05		3.44×10^1

^aIn units of $\text{M}^{-1} \text{s}^{-1}$, at $\mu = 0.5 \text{ M}$ except in 70% Me_2SO where $\mu = 0.25 \text{ M}$.

Table III. Kinetic Parameters for Scheme II

parameter	solvent Me_2SO	BMN-OMe	BMN	BMN-Cl	BMN- NO_2
k_i, s^{-1} ^a	50%		30 ± 5	16 ± 3	7 ± 2
	70%	6 ± 1	5 ± 1	2.5 ± 0.5	1.0 ± 0.2
$K_5^{\text{OH}}K_6^{\text{H}_2\text{O}}, \text{M}^{-1} \text{s}^{-1}$	50%		110 ± 15	190 ± 20	380 ± 40
	70%	40 ± 10	35 ± 7	60 ± 8	133 ± 15
$K_5^{\text{OH}}K_6^{\text{H}_2\text{O}}k_4, \text{s}^{-1}$	50%			74 ± 15	57 ± 7
	70%				~ 13
$k_6^{\text{OH}}/k_4, \text{M}^{-1}$ ^b	50%			2.6 ± 0.8	6.7 ± 1.5
	70%				~ 10.2

^a k_i refers to a concerted intramolecular proton switch with transition state 2; for transition state 3, k_i is replaced by $k_{6i}^{\text{H}}K_a^{\text{OH}}(T_{\text{OH}})$, for transition state 4 by $k_{2i}^{\text{H}_2\text{O}}$ as discussed under Importance and Mechanism of the k_i step. ^b $k_6^{\text{OH}}/k_4 = K_5^{\text{OH}}K_6^{\text{H}_2\text{O}}/K_5^{\text{OH}}K_6^{\text{H}_2\text{O}}k_4$.

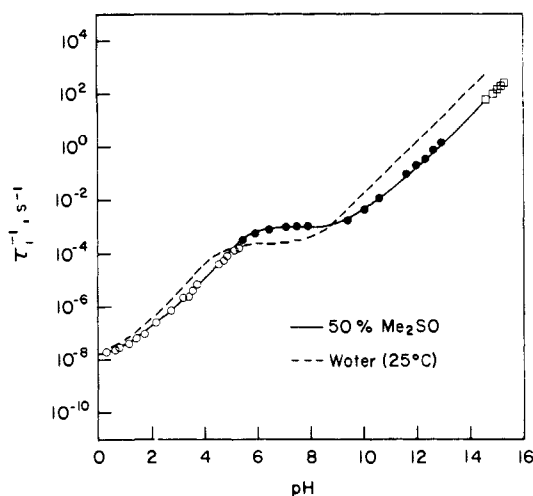


Figure 2. pH-rate profile of τ_1^{-1} for BMN in 50% Me_2SO -50% water at 20 °C: (\square) KOH solutions; (\bullet) buffers; (\circ) data from ref 2b. (---) pH-rate profile of τ_1^{-1} for BMN in water at 25 °C, ref 2a.

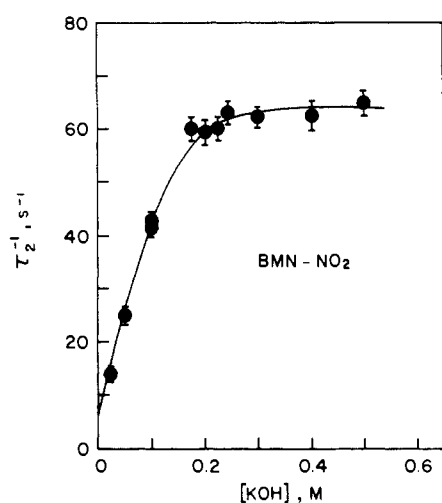


Figure 3. τ_2^{-1} as a function of $[\text{KOH}]$ for BMN- NO_2 in 50% Me_2SO -50% water at 20 °C.

phosphate, and borate buffers (total buffer concentration 0.01–0.02 M) between pH 5.4 and 12.9. At these low buffer concentrations, buffer catalysis ($k_1^{\text{B}}[\text{B}]$) is very weak^{2a} and τ_1^{-1} is given by eq 2.

$$\tau_1^{-1} \approx k_1^{\text{H}_2\text{O}} + k_1^{\text{OH}}[\text{OH}^-] \quad (2)$$

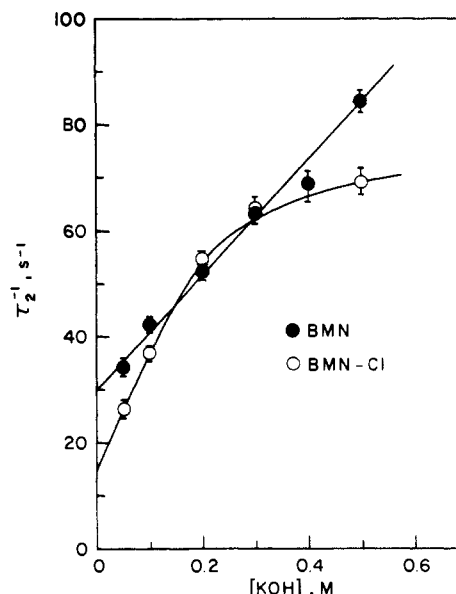


Figure 4. τ_2^{-1} as a function of $[\text{KOH}]$ for BMN and BMN-Cl in 50% Me_2SO -50% water at 20 °C.

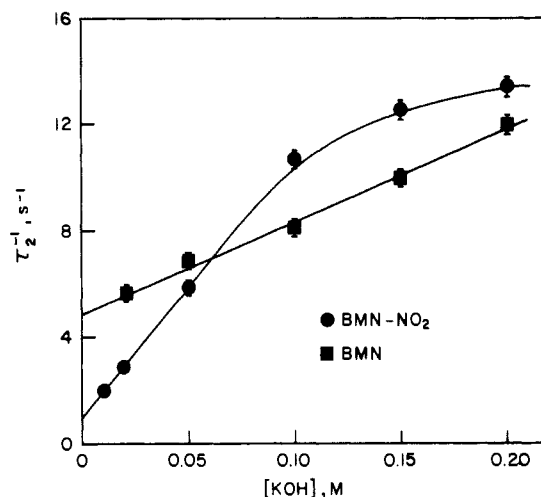


Figure 5. τ_2^{-1} as a function of $[\text{KOH}]$ for BMN- NO_2 and BMN in 70% Me_2SO -30% water at 20 °C.

The results are in Table S6,⁸ while Figure 2 shows a pH-rate profile which also includes the previously published data in acidic solution.^{2b} $k_1^{\text{H}_2\text{O}}$ was obtained from the plateau between pH 6.5 and 9.

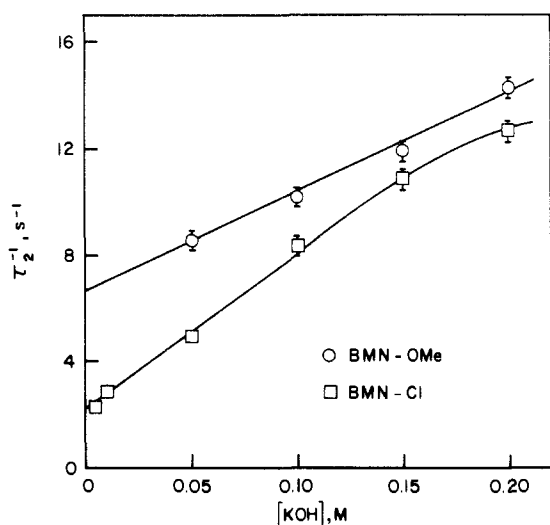
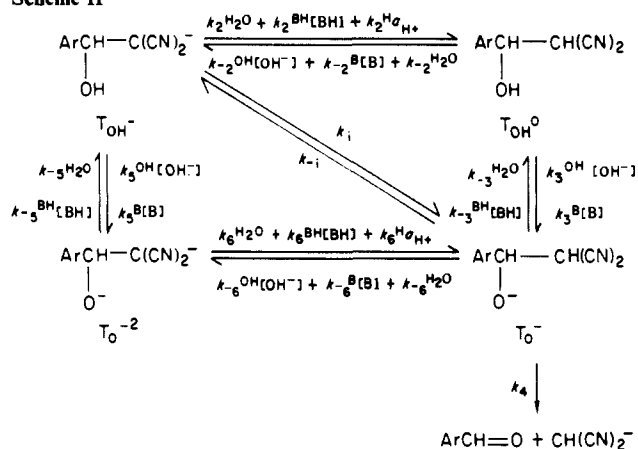


Figure 6. τ_2^{-1} as a function of [KOH] for BMN-Cl and BMN-OMe in 70% Me₂SO–30% water at 20 °C.

Scheme II



Kinetics of Conversion of T_{OH}^- into Products. τ_2^{-1} was measured for selected compounds in 50% and 70% Me₂SO. The results are summarized in Tables S7 and S8,⁸ while Figures 3–6 show plots of τ_2^{-1} vs. [KOH]. Note that the experimental error in the τ_2^{-1} values is significantly larger than in the τ_1^{-1} values, as reflected in the error bars shown in the figures. This is because the OD changes associated with τ_2^{-1} were quite small, as pointed out above.

For BMN-OMe and BMN, τ_2^{-1} shows a linear dependence on [KOH] with a significant intercept. With BMN-NO₂, there is a leveling off at high base concentrations in both solvents, while with BMN-Cl τ_2^{-1} approaches a plateau only in 50% Me₂SO. The probable reason why with this latter substrate there is only very little curvature if any in 70% Me₂SO is that for solubility reasons, the highest [KOH] was only 0.2 M instead of 0.5 M.

Our results can be understood with reference to Scheme II which shows T_{OH}^- as the ground state.⁹

In the absence of a buffer (B, BH) which is the condition under which the τ_2^{-1} values shown in Figures 3–6 were obtained, we can derive an expression for τ_2^{-1} based on the following reasoning.

(1) The fact that τ_2^{-1} increases with increasing base concentration means that the k_4 step cannot be rate-limiting, at least not in the range where τ_2^{-1} depends linearly on [KOH]. This is because base catalysis can only accelerate the formation of T_O^- (k_3^{OH} and/or k_5^{OH} step), a process which already is fast if k_4 is rate limiting.

(2) The base-independent term of τ_2^{-1} (intercepts in Figures 3–6) must be associated with the k_i step and/or the pathway via

T_{OH}^0 , the base-dependent term with the pathway via T_O^{2-} . As will be shown in the Discussion, the contribution of the T_{OH}^0 pathway is negligible unless a buffer is added (see below).

Using the steady-state approximation for T_O^{2-} and T_O^- , we obtain¹⁰ eq 3. The linear increase of τ_2^{-1} with [KOH] can be understood by assuming $k_6^{OH}[OH^-] \ll k_4$ at low [KOH]. Equation 3 then simplifies to eq 4.

$$\tau_2^{-1} = \frac{k_5^{OH}k_6^{H_2O}k_4[OH^-]}{k_{-5}^{H_2O}k_6^{OH}[OH^-] + k_{-5}^{H_2O}k_4 + k_6^{H_2O}k_4} + k_i \quad (3)$$

$$\tau_2^{-1} = \frac{k_5^{OH}k_6^{H_2O}[OH^-]}{k_{-5}^{H_2O} + k_6^{H_2O}} + k_i \quad (4)$$

Since the oxygen basicity of T_O^{2-} must be in the order of that of OH⁻ (see below) we expect $k_{-5}^{H_2O} \gg k_6^{H_2O}$ by many orders of magnitude. Hence, eq 4 reduces further to eq 5 with $K_5^{OH} = k_5^{OH}/k_{-5}^{H_2O}$. The values obtained for $K_5^{OH}k_6^{H_2O}$ and k_i are summarized in Table III.

$$\tau_2^{-1} = K_5^{OH}k_6^{H_2O}[OH^-] + k_i \quad (5)$$

The leveling off for BMN-NO₂ (Figures 3 and 5) and BMN-Cl (Figure 4) may be understood in either of two ways. It could be a consequence of a change from $k_6^{OH}[OH^-] \ll k_4$ to $k_6^{OH}[OH^-] \gg k_4$. Coupled with $k_{-5}^{H_2O} \gg k_6^{H_2O}$ (see above), this would reduce eq 3 to eq 6 with $K_6^{H_2O} = k_6^{H_2O}/k_6^{OH}$.

$$\tau_2^{-1} = K_5^{OH}K_6^{H_2O}k_4 + k_i \quad (6)$$

The second possibility is that T_O^{2-} accumulates at high base concentrations and eventually becomes a new ground state. If the $T_{OH}^- + OH^- \rightleftharpoons T_O^{2-}$ reaction is treated as a rapid equilibrium, the expression for τ_2^{-1} becomes eq 7.

$$\tau_2^{-1} = \frac{K_5^{OH}k_6^{H_2O}[OH^-] + k_i}{1 + K_5^{OH}[OH^-]} \quad (7)$$

At low base concentration ($K_5^{OH}[OH^-] \ll 1$), eq 7 is equivalent to eq 5, while at high concentrations ($K_5^{OH}[OH^-] \gg 1$) it becomes eq 8.

$$\tau_2^{-1} = k_6^{H_2O} + \frac{k_i}{K_5^{OH}[OH^-]} \approx k_6^{H_2O} \quad (8)$$

As will be shown in the Discussion the first possibility is more likely and the parameters listed in Table II ($K_5^{OH}K_6^{H_2O}k_4$, k_6^{OH}/k_4) are based on eq 6.

General Acid Catalyzed Conversion of T_{OH}^- into Products.

Further evidence for the assignment of rate-limiting steps in Scheme II was sought by studying general acid catalysis. Several problems needed to be overcome to attain this goal.

At the pH values required to see the τ_2^{-1} process, there are no convenient buffers which have a high enough pK_a^{BH} for significant concentrations of BH to be present (e.g., amines) or whose spectral properties do not interfere with the observation of the reaction (e.g., phenols).

Even if such buffers were available and added to the reaction solutions before the formation of T_{OH}^- is complete, competing nucleophilic attack on the olefin would seriously interfere with our measurements.^{6b,11} What is required is that T_{OH}^- be generated at high [KOH] in the absence of buffer. At this point a buffer solution at significantly lower pH must be added. This addition has to occur before the τ_2^{-1} process has made significant process, i.e., within 50–100 ms (depending on substrate and solvent) after mixing the olefin with KOH.

We were able to carry out such experiments with a piperidine buffer at pH 10.8 in a three-way mixing device of our stopped-flow apparatus (see Experimental Section). We chose the BMN-OMe system in 70% Me₂SO because the ΔOD associated with τ_2^{-1} is largest and gives the most accurate results. These are summarized in Table S9,⁸ while Figure 7 shows a plot of τ_2^{-1} vs. piperidinium

(9) That the equilibrium $S \rightleftharpoons T_{OH}^-$ is virtually completely on the side of T_{OH}^- at high base concentrations in aqueous solution has been shown previously.² That T_{OH}^- is even more favored in Me₂SO-containing solvents will be shown in the Discussion.

(10) Strictly speaking, the term for the k_i pathway is $k_i k_4 / (k_{-1} + k_4)$. However, as stated above, observation of strong base catalysis implies that k_4 cannot be strongly co-rate-limiting and hence $k_4 \gg k_{-1}$.

(11) Bernasconi, C. F.; Fox, J. P.; Fornarini, S. *J. Am. Chem. Soc.* **1980**, *102*, 2810.

Table IV. Summary of Rate and Equilibrium Constants of the Steps in Scheme I for BMN in Four Solvents

no.	parameter	water	Me ₂ SO		
			50%	60%	70%
Step 1					
1	$K_1^{H_2O}$, M	$\sim 1.29 \times 10^{-11}$	$\sim 2.92 \times 10^{-10}$	$\sim 7.90 \times 10^{-10}$	$\sim 9.50 \times 10^{-10}$
2	$k_1^{H_2O}$, s ⁻¹	1.21×10^{-4}	1.05×10^{-3}		
3	k_2^H , M ⁻¹ s ⁻¹	$\sim 9.4 \times 10^6$	$\sim 3.5 \times 10^6$		
4	K_1^{OH} , M ⁻¹	$\sim 1.29 \times 10^3$	$\sim 2.32 \times 10^6$	$\sim 3.70 \times 10^7$	$\sim 5.86 \times 10^8$
5	k_1^{OH} , M ⁻¹ s ⁻¹	1.26×10^2	1.00×10^3	2.30×10^3	6.75×10^3
6	$k_2^{H_2O}$, s ⁻¹	$\sim 9.77 \times 10^{-2}$	$\sim 4.31 \times 10^{-4}$	$\sim 6.22 \times 10^{-5}$	$\sim 1.15 \times 10^{-5}$
7	$K_1^{H_2O}/K_a^{CH}$	$\sim 1.0 \times 10^{-2}$	$\sim 1.5 \times 10^{-2}$	$\sim 2.8 \times 10^{-2}$	$\sim 2.5 \times 10^{-2}$
Step 2					
8	$pK_a^{CH}(T_{OH}^0)^a$	~ 8.89	~ 7.71	~ 7.55	~ 7.42
9	$k_2^{H_2O}$, s ⁻¹	~ 6.2	$\geq 1.04 \times 10^{-2}$		$\geq 1.0 \times 10^{-3}$
10	k_3^{OH} , M ⁻¹ s ⁻¹	$\sim 8.0 \times 10^5$	$\geq 1.6 \times 10^6$		$\geq 2.4 \times 10^7$
11	k_3^H , M ⁻¹ s ⁻¹	$\sim 2 \times 10^9$	$\sim 2 \times 10^9$	$\sim 2 \times 10^9$	$\sim 2 \times 10^9$
12	$k_2^{H_2O}$, s ⁻¹	~ 2.6	$\sim 3.9 \times 10^1$	$\sim 5.6 \times 10^1$	$\sim 7.6 \times 10^1$
13	$pK_a^{CH_2(CN)_2}$	11.39	10.21	10.05	9.92
Step 3					
14	$pK_a^{OH}(T_{OH}^0)^b$	~ 11.1	~ 13.0	~ 13.8	~ 14.7
15	k_3^{OH} , M ⁻¹ s ⁻¹	$\sim 2 \times 10^9$	$\sim 1.5 \times 10^9$	$\sim 1.5 \times 10^9$	$\sim 1.5 \times 10^9$
16	$k_3^{H_2O}$, s ⁻¹	$\sim 3.5 \times 10^6$	$\sim 2.0 \times 10^6$	$\sim 2.0 \times 10^6$	$\sim 1.2 \times 10^6$
17	$k_3^{H_2O}$, s ⁻¹	$\sim 3.2 \times 10^{-1}$	$\sim 1 \times 10^{-3}$	$\sim 1.2 \times 10^{-4}$	$\sim 8 \times 10^{-6}$
18	k_3^H , M ⁻¹ s ⁻¹	$\sim 4 \times 10^{10}$	$\sim 1 \times 10^{10}$	$\sim 0.75 \times 10^{10}$	$\sim 0.40 \times 10^{10}$
19	pK_w	14.00	15.90	16.67	17.79
Step 34					
20	$K_4^{H_2O}$, M	~ 0.33	$\sim 6.9 \times 10^{-2}$		$\sim 3.25 \times 10^{-2}$
21	$k_4^{H_2O}$, s ⁻¹	$\sim 1.0 \times 10^{-6}$	$\sim 1.05 \times 10^{-6}$		$\sim 4.76 \times 10^{-7}$
22	$k_{-4}^{H_2O}$, M ⁻¹ s ⁻¹	3.0×10^{-6}	$\sim 1.52 \times 10^{-5}$		$\sim 1.46 \times 10^{-5}$
Step 4					
23	K_4 , M	$\sim 2.1 \times 10^{-1}$	$\sim 4.3 \times 10^1$	$\sim 2.0 \times 10^2$	$\sim 2.0 \times 10^3$
24	k_4 , s ⁻¹	$\sim 3.3 \times 10^4$	$\sim 5.9 \times 10^5$	$\sim 1.6 \times 10^6$	$\sim 5.9 \times 10^6$
25	k_{-4} , M ⁻¹ s ⁻¹	$\sim 1.5 \times 10^5$	$\sim 1.4 \times 10^4$	$\sim 7.9 \times 10^3$	$\sim 3.0 \times 10^3$

^a $K_a^{CH}(T_{OH}^0) = (K_2^{H_2O})^{-1} = k_2^{H_2O}/k_2^H$. ^b $K_a^{OH}(T_{OH}^0) = K_3^{H_2O} = k_3^{H_2O}/k_3^H$.

ion concentration. That the observed catalysis is indeed general acid catalysis was shown by the absence of significant catalysis at pH 12.0; this pH is still below the pH range in which the T_O^{2-} pathway contributes and where general base catalysis could, in principle, be observable. Hence, the plot of Figure 7 can be described by eq 9 with $k_2^{BH} = 2.92 \times 10^3 \text{ M}^{-1} \text{ s}^{-1}$.

$$\tau_2^{-1} = k_2^{BH}[\text{BH}] + k_i \quad (9)$$

Dissection of Rate and Equilibrium Constants. Table IV summarizes the rate and equilibrium constants of all steps shown in Scheme I (except for the general base and acid terms) for the parent BMN in four different solvents. The parameters for steps, 3, 34, and 4 were obtained previously from data in acidic solution.^{2b} The parameters for steps 1 and 2 were measured or estimated as follows.

(1) k_1^{OH} and $k_1^{H_2O}$ were measured directly (eq 1 and 2).

(2) The $pK_a^{CH}(T_{OH}^0)$ was estimated as $pK_a^{CH_2(CN)_2} - 2.5$ from the known $pK_a^{CH_2(CN)_2}$ values of malononitrile; 2.5 is the approximate difference between $pK_a^{CH_2(CN)_2}$ and $pK_a^{CH}(T_{OH}^0)$ in aqueous solution, based on a measured $pK_a^{CH}(T_{Mor}^0)$ for the morpholine adduct of BMN.²⁴

(3) From the $K_1^{H_2O}/K_a^{CH}$ ratios determined in acidic solution^{2b} (entry 7 in Table IV) $K_1^{H_2O}$ and $K_1^{OH} = K_1^{H_2O}/K_w$ were calculated. Coupled with $k_1^{H_2O}$ and k_1^{OH} , we then obtained k_{-1}^H and $k_{-1}^{H_2O}$, respectively.

(4) For k_2^H , we used Hibbert's¹² value of $2 \times 10^9 \text{ M}^{-1} \text{ s}^{-1}$ determined in water for all solvents, while $k_{-2}^{H_2O}$ was found in combination with $pK_a^{CH}(T_{OH}^0)$.

(5) $k_2^{H_2O}$ and k_2^{OH} were the most difficult to estimate. Malononitriles behave very much like normal acids in that the rate constants for thermodynamically favored deprotonation by general bases are essentially independent of the pK_a of the base, although they do not quite reach the diffusion-controlled limit.¹² However, the hydroxide ion deviates from this behavior in that

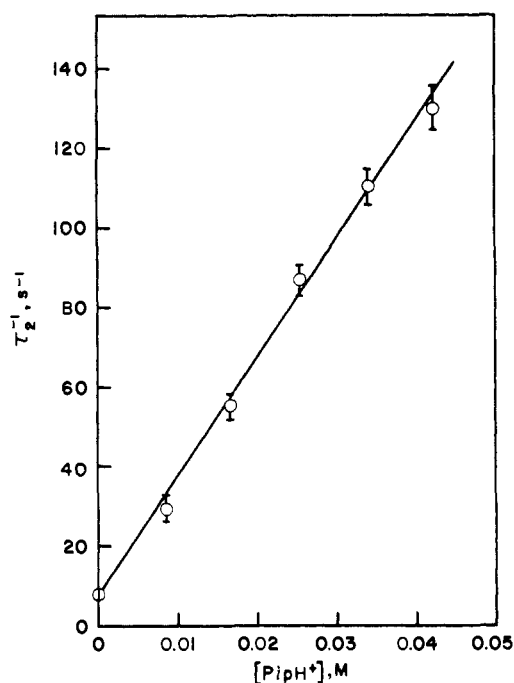


Figure 7. τ_2^{-1} as function of piperidinium ion concentration for BMN-OME in 70% Me₂SO-30% water at 20 °C. Experiments in three-way mixing stopped-flow apparatus.

it reacts with a much lower rate constant ($<10^6 \text{ M}^{-1} \text{ s}^{-1}$) than the weaker bases. In aqueous solution, we^{2a} recently estimated $k_{-2}^{OH} \approx 8 \times 10^5 \text{ M}^{-1} \text{ s}^{-1}$ on the basis of Hibbert's work.¹²

Since the low reactivity of hydroxide ion in water is probably caused by its strong solvation,¹³ one expects that k_{-2}^{OH} in the Me₂SO-containing solvents is enhanced. The values for k_{-2}^{OH}

(12) (a) Hibbert, F.; Long, F. A.; Walters, E. A. *J. Am. Chem. Soc.* **1971**, *93*, 2829. (b) Hibbert, F. *Compr. Chem. Kinet.* **1977**, *8*, 97.

(13) Kresge, A. J. *Chem. Soc. Rev.* **1973**, *2*, 475.

Table V. Kinetic Parameters for Scheme II based on Alternative Interpretation (Equation 8)^a

parameter	solvent Me ₂ SO	BMN-Cl	BMN-NO ₂
$k_6^{H_2O}$, s ⁻¹	50% 70%	90 ± 12	65 ± 5 ~14
K_5^{OH} , M ⁻¹	50% 70%	2.1 ± 0.5	5.8 ± 1.2 ~9.5

^aSee text.

given in Table IV are estimated based on a method presented in the Discussion.

In Table III, we have summarized the kinetic parameters which refer to Scheme II. With reference to Figures 3–6, k_i is the intercept, $K_5^{OH}k_6^{H_2O}$ is the slope, $K_5^{OH}K_6^{H_2O}k_4$ is plateau minus intercept, while k_{-6}^{OH}/k_4 is $K_5^{OH}k_6^{H_2O}/K_5^{OH}K_6^{H_2O}k_4$.

Discussion

Mechanism in Water. In water the rate of disappearance of BMN-X and the rates of formation of ArCH=O and CH(CN)₂⁻ are the same for all X, irrespective of pH. This indicates that none of the intermediates shown in Scheme I or Scheme II accumulates to detectable levels. Different steps are rate-limiting depending on the pH, but in basic and neutral solution, which is the focus of this paper, it is always formation of T_{OH}⁻ by OH⁻ or water attack on the olefin which is rate-limiting.^{2a}

With an estimated $K_1^{OH} \approx 1.29 \times 10^3$ M⁻¹ for the equilibrium constant of OH⁻ addition to the parent BMN (Table IV), it is apparent that at high base concentrations, $K_1^{OH}[\text{OH}^-] \gg 1$. This means that T_{OH}⁻ is thermodynamically strongly favored over BMN. Hence, the reason why T_{OH}⁻ does not accumulate in water is not instability relative to the reactants but a high rate of conversion of T_{OH}⁻ to products.

It is noteworthy, though, that carbon protonation of T_{OH}⁻ by water ($k_2^{H_2O}$) is much too slow to account for this rapid conversion to products. For example, at 0.5 M KOH, the highest concentration used, $k_1^{OH}[\text{OH}^-] = 63$ s⁻¹, while $k_2^{H_2O}$ is estimated at 6.2 s⁻¹ (Table IV). This indicates the availability of more effective pathways for conversion of T_{OH}⁻ to products, as shown in Scheme II, i.e., we must have $k_i + K_5^{OH}k_6^{H_2O}[\text{OH}^-] \gg 63$ s⁻¹ at [KOH] = 0.5 M.

Mechanism in Me₂SO–Water Mixtures. In the mixed solvents, T_{OH}⁻ does accumulate and increasingly so as the Me₂SO content increases. This allowed us to study the kinetics of the conversion of T_{OH}⁻ into products (τ_2^{-1}) separately. From the dependence of τ_2^{-1} on base concentration, it is clear that both the pathway via T_O²⁻ and the intramolecular proton-transfer (k_i) pathway contribute.

The increased separation between τ_1^{-1} and τ_2^{-1} with increasing Me₂SO content, and with it the better measurability of τ_2^{-1} , is the combined result of the rate-enhancing effect on k_1^{OH} (Table II) and the decrease in k_i and $K_5^{OH}k_6^{H_2O}$ (Table III). Electron-withdrawing substituents further enhance k_1^{OH} (Table II) and decrease the rate of product formation.

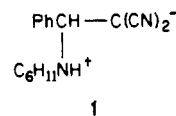
The leveling off in some of the plots of τ_2^{-1} vs. [KOH] (Figures 3–5) was attributed to a change from $k_{-6}^{OH}[\text{OH}^-] \ll k_4$ to $k_{-6}^{OH}[\text{OH}^-] \gg k_4$ at high base concentrations which leads to eq 6. We now present arguments which show this to be a more reasonable interpretation than to assume that T_O²⁻ becomes a new ground state (eq 7 and 8).

Table V lists the parameters which one would obtain from eq 8 ($k_6^{H_2O}$) and from the ratio of slope/plateau ($K_5^{OH}k_6^{H_2O}/k_6^{H_2O} = K_5^{OH}$). Using $\rho \approx 1.0$, one estimates $K_5^{OH} \sim 1.0$ and ~ 1.5 for BMN in 50% and 70% Me₂SO, respectively. These numbers translate into $pK_a^{OH}(\text{T}_{OH}^-) \approx 15.9$ in 50% Me₂SO and ≈ 17.6 in 70% Me₂SO. In combination with $pK_a^{OH}(\text{T}_{OH}^0)$ and $pK_a^{CH}(\text{T}_{OH}^0)$, we can then also estimate $pK_a^{CH}(\text{T}_{O}^-)$ from eq 10. We obtain $pK_a^{CH}(\text{T}_{O}^-) \approx 10.6$ in 50% and 10.3 in 70% Me₂SO.

$$pK_a^{CH}(\text{T}_{O}^-) = pK_a^{CH}(\text{T}_{OH}^0) + pK_a^{OH}(\text{T}_{OH}^-) - pK_a^{OH}(\text{T}_{OH}^0) \quad (10)$$

Two lines of reasoning suggest that these $pK_a^{OH}(\text{T}_{OH}^-)$ and $pK_a^{CH}(\text{T}_{O}^-)$ values are too low to be realistic. (1) Since the calculated $pK_a^{OH}(\text{T}_{OH}^-)$ is close to pK_w (entry 19 in Table IV)

and hence more than one pK unit below the pK_a of water, this implies that substituting one hydrogen of water with the PhCH(CN)₂⁻ moiety has an acidifying effect of more than one pK unit. In comparison, the pK_a^{NH} of **1** is approximately 0.7 units lower than the pK_a of the piperidinium ion.¹¹ Most of this latter



pK_a difference can probably be accounted for by the fact that the conjugate base of **1** is a tertiary amine whose basicity is expected to be lower than for a secondary amine.¹⁴ In other words, the PhCH(CN)₂⁻ moiety does not appear to be significantly electron-withdrawing and may even be somewhat electron-donating. It is therefore difficult to explain why $pK_a^{OH}(\text{T}_{OH}^-)$ should be so low.

(2) The calculated $pK_a^{CH}(\text{T}_{O}^-)$ values allow us to estimate k_{-6}^{OH} in 50% and 70% Me₂SO as follows. We first estimate $k_6^{H_2O}$ for the parent BMN to be ≈ 360 s⁻¹ in 50% Me₂SO and ≈ 85 s⁻¹ in 70% Me₂SO, based on $k_6^{H_2O}$ for BMN-NO₂ (Table V) and a $\rho \approx 1.0$. In conjunction with $pK_a^{CH}(\text{T}_{O}^-)$, this affords $k_{-6}^{OH} \approx 7.1 \times 10^7$ M⁻¹ s⁻¹ in 50% and $k_{-6}^{OH} \approx 2.6 \times 10^9$ M⁻¹ s⁻¹ in 70% Me₂SO. These k_{-6}^{OH} values are ≈ 90 - and ≈ 3250 -fold higher than k_{-2}^{OH} in water. Even though the reduced solvation of OH⁻ in the Me₂SO-containing solvents is expected to enhance k_{-6}^{OH} (see discussion under the heading Dissociation of Rate and Equilibrium Constants), the factors of ≈ 90 and ≈ 3250 , respectively, seem unrealistically high. These factors would be correspondingly reduced if $pK_a^{CH}(\text{T}_{O}^-)$ were higher.

Estimates for k_{-6}^{OH} , k_{-2}^{OH} , and k_{-2}^B . More reasonable estimates for k_{-6}^{OH} emerge from the interpretation of the leveling off in terms of eq 6 which affords the k_{-6}^{OH}/k_4 ratios summarized in Table III.

For the parent BMN, $k_4 \approx 5.9 \times 10^5$ s⁻¹ in 50% Me₂SO and $\approx 5.9 \times 10^6$ s⁻¹ in 70% Me₂SO (Table IV). Assuming a $\rho \approx -0.5$ for the substituent effect on k_4 leads to $k_4 \approx 2.4 \times 10^5$ and $\approx 2.4 \times 10^6$ s⁻¹ for BMN-NO₂ in the two solvents. This then leads to $k_{-6}^{OH} \approx 1.6 \times 10^6$ M⁻¹ s⁻¹ in 50% and $k_{-6}^{OH} \approx 2.4 \times 10^7$ M⁻¹ s⁻¹ in 70% Me₂SO; i.e., the enhancement over $k_{-2}^{OH} \approx 8 \times 10^5$ M⁻¹ s⁻¹ in water is ≈ 2.0 -fold and ≈ 30 -fold, respectively.

In estimating k_{-2}^{OH} in 50% and 70% Me₂SO (Table IV), we have adopted the k_{-6}^{OH} values as lower limits since k_{-2}^{OH} does not suffer from the electrostatic repulsion of two negative charges.

From $k_2^{BH} = 2.92 \times 10^3$ M⁻¹ s⁻¹ for the protonation of T_{OH}⁻ derived from BMN-OMe by piperidinium ion in 70% Me₂SO, we calculate $k_{-2}^B \approx 3 \times 10^6$ M⁻¹ s⁻¹ for the proton transfer in the thermodynamically favorable reverse direction.¹⁵ This compares with a value of $\approx 2 \times 10^7$ M⁻¹ s⁻¹ in water at 25 °C for the proton transfer between CHBr(CN)₂ and morpholine in the thermodynamically favorable direction.¹⁶ The somewhat lower value in our system is probably the combined result of a steric effect due to the bulkiness of the PhCH(OH) moiety, the stronger solvation of the protonated amine in the Me₂SO-containing solvent,¹⁷ and the lower temperature.

Importance and Mechanism of the k_i Step. It is noteworthy that the intramolecular proton switch, T_{OH}⁻ → T_O⁻, is so much faster than carbon protonation of T_{OH}⁻ by water. For example, for BMN we have $k_i/k_2^{H_2O} \leq 2.9 \times 10^3$ in 50% Me₂SO and $\leq 5.0 \times 10^3$ in 70% Me₂SO (k_i from Table III, $k_2^{H_2O}$ from Table IV). This contrasts with the hydrolysis of 1,1-dinitro-2,2-diphenylethylene,⁷ benzylidene Meldrum's acid,^{6b} and benzylidene-1,3-indandione¹⁸ where the intramolecular pathway could not even be detected.

(14) For example, for piperidine → N-methylpiperidine, the pK is lowered by about one unit: Searles, S.; Tamres, M.; Block, F.; Quaterman, L. A. *J. Am. Chem. Soc.* **1956**, *78*, 4917.

(15) $pK_a^{CH}(\text{T}_{OH}^0)$ for BMN-OMe is estimated to be 0.77 units higher than that for BMN (7.42, Table IV), based on an estimated $\rho \approx 1.0$.

(16) Hibbert, F.; Long, F. A. *J. Am. Chem. Soc.* **1972**, *94*, 2647.

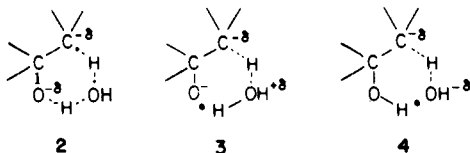
(17) Bernasconi, C. F. *Tetrahedron* **1985**, *41*, 3219.

(18) Bernasconi, C. F.; Laibelman, A.; Zitomer, J. L. *J. Am. Chem. Soc.* **1985**, *107*, 6563.

One factor which probably contributes to this result is that $pK_a^{OH}(T_{OH}^0)$ is significantly lower in the BMN system than in these other systems. It was shown previously that the relative importance of the intramolecular compared to the intermolecular pathway increases when the pK_a of the donor group (OH group in the present case) decreases toward the midrange of the pK_a scale.¹⁹

A second, probably even more important, factor is that the deprotonation of malononitrile by OH^- (protonation of the anion by water) is unusually slow relative to the general base/acid-promoted proton transfers,¹² as commented upon earlier. In other words, the $k_i/k_2^{H_2O}$ ratios are high because of low $k_2^{H_2O}$ values rather than because of unusually large k_i values.

The most likely mechanism of the k_i step is a concerted proton transfer with a transition state that includes a water bridge (2).¹⁹



Two kinetically equivalent alternatives are shown in 3 and 4. 3 represents carbon protonation of T_{O}^{2-} by H_3O^+ with transition-state stabilization by hydrogen bonding and electrostatic interaction between O^- and H_3O^+ in 3. The rate constant for conversion of T_{OH}^- to T_{O}^- (Scheme II) would then not be k_i but be given by $k_{6i}^H K_a^{OH}(T_{OH}^-)$, with $K_a^{OH}(T_{OH}^-)$ being the acidity constant of T_{OH}^- and k_{6i}^H being the rate constant for carbon protonation of T_{O}^{2-} by H_3O^+ (see footnote a in Table III); we use the symbol k_{6i}^H rather than k_6^H (Scheme II) in order to indicate the intramolecular assistance by hydrogen bonding and electrostatic interaction which is not present in the simple, unassisted k_6^H step.

4 indicates carbon protonation of T_{OH}^- by water with transition-state stabilization by hydrogen bonding to the incipient hydroxide ion. In this case, the rate constant for the rate-limiting step in the conversion of T_{OH}^- to T_{O}^- would be $k_{2i}^{H_2O}$ (footnote a in Table III); the subscript i is again used to distinguish this intramolecularly assisted pathway from the unassisted $k_2^{H_2O}$ step in Scheme II.

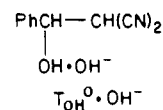
A transition state similar to 3 was suggested by Jencks²⁰ in order to explain the exalted rate constant for carbon protonation of acetone enolate ion by H_3O^+ . This mechanism is, however, not viable in our system because it requires an unreasonably high value for k_{6i}^H . On the basis of $k_{6i}^H K_a^{OH}(T_{OH}^-) = 30 \text{ s}^{-1}$ (see Table III and footnote a in the table), $pK_a^{OH}(T_{OH}^-) \geq 15.9$ in 50% Me_2SO , and $k_{6i}^H K_a^{OH}(T_{OH}^-) = 5.0 \text{ s}^{-1}$ and $pK_a^{OH}(T_{OH}^-) \geq 17.6$ in 70% Me_2SO for BMN, one calculates $k_{6i}^H \geq 2.4 \times 10^{17} \text{ M}^{-1} \text{ s}^{-1}$ in 50% Me_2SO and $k_{6i}^H \geq 1.26 \times 10^{18} \text{ M}^{-1} \text{ s}^{-1}$ in 70% Me_2SO . These values are many orders of magnitude higher than the rate constants for a diffusion-controlled reaction and thus 3 is safely excluded.

It should be noted that exclusion of 3 for the BMN adduct does not necessarily invalidate Jencks' proposal in the acetone enolate reaction. In the enolate ion, the oxygen and carbon are part of a resonance system, and protonation at one site has a very much larger effect on the pK_a of the other site than in our system. This could have a significant influence on the mechanism.

That transition state 4 is also unattractive can be seen as follows. The $k_{2i}^{H_2O}$ value (see Table III and footnote a in that table) for BMN is $\leq 2.9 \times 10^3$ times larger than $k_2^{H_2O}$ (Table IV) in 50% Me_2SO and $\leq 5.0 \times 10^3$ times larger than $k_2^{H_2O}$ in 70% Me_2SO . This indicates that hydrogen-bonding stabilization of the transition state would have to be very strong. Since the pK difference between the hydrogen bond donor and acceptor site in 4 cannot be very large, such strong stabilization is unlikely.

We can cast this argument into a more quantitative form by first estimating the hydrogen-bonding stabilization of $T_{OH}^0 \cdot OH^-$

which would be the product of the $k_{2i}^{H_2O}$ step. According to the



Hine²¹ equation, the association constant for a hydrogen-bonded complex $AH \cdot B$ is given by eq 11. The first term on the right represents the enhancement of $K_{AH \cdot B}$ over a situation where $AH \cdot B$ is simply an encounter complex without hydrogen bonding and has a $\log K_{AH \cdot B} = -(\log [H_2O])$.

$$\log K_{AH \cdot B} = \tau(pK_{H_3O^+} - pK_{BH})(pK_{AH} - pK_{H_2O}) - \log [H_2O] \quad (11)$$

When applied to $T_{OH}^0 \cdot OH^-$ in 50% Me_2SO ($pK_{BH} = pK_{H_2O} = 17.33$, $pK_{AH} = pK_a^{OH}(T_{OH}^0) \approx 13.0$, $pK_{H_3O^+} = -1.43$) and Jencks'²² value of 0.013 for τ was used, one calculates $K_{AH \cdot B} = 0.43$. This represents a 11.5-fold enhancement over $K_{AH \cdot B}$ in the absence of hydrogen bonding. If this effect was entirely carried over into the transition state (4), it would mean a 11.5-fold enhancement of $k_{2i}^{H_2O}$ over $k_2^{H_2O}$. However, in 4, pK_{BH} must be lower than pK_{H_2O} and pK_{AH} should be higher than $pK_a^{OH}(T_{OH}^0)$, and thus $k_{2i}^{H_2O}/k_2^{H_2O}$ should be $\ll 11.5$. For example, if pK_{BH} dropped to 12.0 and pK_{AH} increased to 14.5, the $k_{2i}^{H_2O}/k_2^{H_2O}$ ratio would be reduced to 3.12. A larger $k_{2i}^{H_2O}/k_2^{H_2O}$ ratio would be conceivable if τ in 50% Me_2SO was significantly larger than in water. However, in order to account for the observed $k_{2i}^{H_2O}/k_2^{H_2O}$ ratio in the order of 10^3 , τ would have to be ≈ 0.78 for the pK_{AH} and pK_{BH} assumed in our example. This is completely unrealistic.^{21,22}

Substituent and Solvent Effects on k_i and $K_5^{OH}k_6^{H_2O}$. In view of the relatively large experimental uncertainties in these parameters and the limited number of substrates amenable to study, we shall only offer a qualitative discussion. k_i is seen to decrease significantly when X becomes more electron withdrawing (Table III). Since a more electron-withdrawing substituent simultaneously increases the OH acidity of T_{OH}^- (k_i -enhancing) and decreases its C basicity (k_i -depressing), the observed decrease in k_i indicates a greater sensitivity to this latter factor. This is not unexpected since the better solvated charge on oxygen is expected to require less stabilization by substituents than the poorly solvated charge on the carbanion; i.e., $K_i = k_i/k_{-i} = K_a^{OH}(T_{OH}^0)/K_a^{CH-}(T_{OH}^0)$ should decrease with more electron-withdrawing substituents.

In contrast to k_i , $K_5^{OH}k_6^{H_2O}$ increases for more electron-withdrawing X. Here the acidifying effect on the OH group (K_5^{OH}) overcompensates for the rate-retarding effect on $k_6^{H_2O}$ which arises from the lower C basicity, apparently because the enhanced acidity of the OH group is fully developed (preequilibrium) but the latter is only partially developed in the transition state.

The solvent effect on both k_i and $K_5^{OH}k_6^{H_2O}$ is obviously dominated by the strong decrease in the OH acidity of T_{OH}^- in the Me_2SO -richer solvent. This decrease is expected to parallel the decrease in the OH acidity of T_{OH}^0 which amounts to ~ 1.7 pK units for 50% \rightarrow 70% Me_2SO (Table IV). In contrast, the solvent effect on the carbon basicity of T_{OH}^- is very weak, with $pK_a^{OH-}(T_{OH}^0)$ decreasing ~ 0.3 units for 50% \rightarrow 70% Me_2SO (Table IV).

Substituent Effects on k_1^{OH} . Figure 8 shows Hammett plots for k_1^{OH} in water and in 50% and 70% Me_2SO . The plots in 30% and 60% Me_2SO have been omitted from the figure for clarity; they look very similar to the ones displayed.

As is apparent from Figure 8, the points for BMN-OMe and BMN-NMe₂ deviate negatively when the standard σ values are used but deviate positively when they are correlated with Brown's σ^+ values²³ (filled symbols). This indicates that the resonance

(21) Hine, J. J. *J. Am. Chem. Soc.* 1972, 94, 5766.

(22) (a) Funderburk, L. H.; Jencks, W. P. *J. Am. Chem. Soc.* 1978, 100, 6708. (b) This value has now also been confirmed experimentally: Jencks, W. P., personal communication.

(23) Brown, H. C.; Okamoto, Y. *J. Am. Chem. Soc.* 1958, 80, 4979.

(19) Bernasconi, C. F.; Hibdon, S. A.; McMurry, S. E. *J. Am. Chem. Soc.* 1982, 104, 3459.

(20) Tapuhi, E.; Jencks, W. P. *J. Am. Chem. Soc.* 1982, 104, 5758.

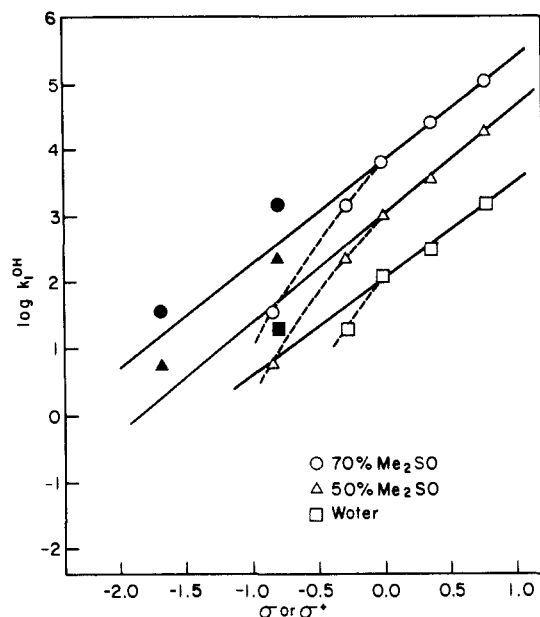


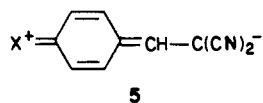
Figure 8. Hammett plots for k_1^{OH} : (open symbols) standard σ ; (filled symbols) σ^+ .

Table VI. $\rho(k_1^{\text{OH}})$ Values as a Function of Solvent and $\beta_{\text{nuc, sol}}$ Values as a Function of Substituent

solvent	$\log \gamma_{\text{OH}}^a$	$\rho(k_1^{\text{OH}})$	substituent	σ^b	$\beta_{\text{nuc, sol}}$
water	0	1.39 ± 0.17	4-NO ₂	0.78	0.34 ± 0.01
30% Me ₂ SO	1.75	1.27 ± 0.09	3-Cl	0.37	0.33 ± 0.01
50% Me ₂ SO	3.25	1.63 ± 0.06	H	0	0.30 ± 0.02
60% Me ₂ SO	4.25	1.56 ± 0.21	4-OMe	-0.27	0.32 ± 0.01
70% Me ₂ SO	5.54	1.56 ± 0.02			

^a Reference 31. ^b Reference 20.

effect which can be attributed to a stabilization of the reactant state (**5**) is appreciable but not as strong as in the system used to define σ^+ .²³



In situations like this, it is often appropriate to analyze the data in terms of the Yukawa-Tsuno²⁴ equation (eq 12) which in our case would yield $1 > r^+ > 0$. Our results are too limited, though, to warrant such quantitative analysis. An added problem is that

$$\log(k/k_0) = \rho(\sigma^n + r^+(\sigma^+ - \sigma^n)) \quad (12)$$

k_1^{OH} for BMN-NMe₂ is disproportionately depressed compared to k_1^{OH} for BMN-OMe. This would lead to a rather uncertain r^+ value and appreciable scatter in the plots according to eq 12. We shall therefore use $\rho(k_1^{\text{OH}})$ calculated on the basis of the standard σ values for H, 3-Cl, and 4-NO₂ (and 4-CN where available) as a measure of the polar effect in our further discussion and deal with the resonance effect of the 4-OMe and 4-NMe₂ substituents in terms of their negative deviations from the Hammett plots.

The $\rho(k_1^{\text{OH}})$ values are in the order of 1.4–1.6 (Table VI). The positive sign is reasonable for a reaction in which there is a rehybridization of the α -carbon from sp^2 to sp^3 ²⁵ and development of negative charge on the substrate. However, in the absence of a ρ value for the equilibrium constant, $\rho(K_1^{\text{OH}})$, the magnitude of $\rho(k_1^{\text{OH}})$ gives little information about the progress of this rehybridization and charge development in the transition state.

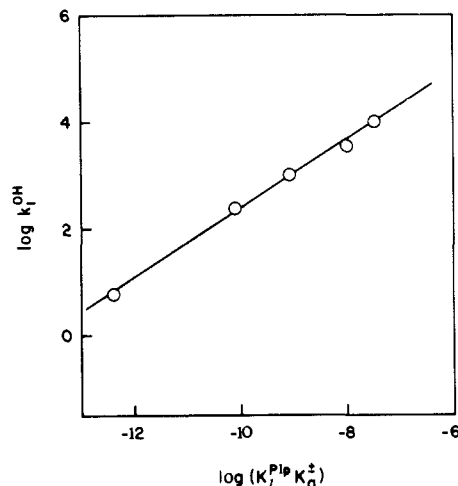
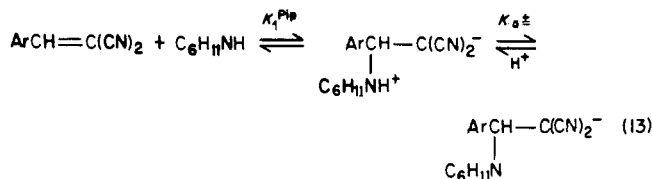


Figure 9. Plot of $\log k_1^{\text{OH}}$ vs. $\log (K_1^{\text{Pip}}K_a^{\pm})$ for the 4-CN, 3-Cl, parent, 4-OMe, and 4-NMe₂ derivatives in 50% Me₂SO–50% water.

As an approximation for $\rho(K_1^{\text{OH}})$, one may use $\rho(K_1^{\text{Pip}}K_a^{\pm})$ ^{26,27} for reaction 13. In 50% Me₂SO, $\rho(K_1^{\text{Pip}}K_a^{\pm}) = 2.43$.²⁶ Hence, we obtain $\rho_{\text{nor}} \approx \rho(k_1^{\text{OH}})/\rho(K_1^{\text{Pip}}K_a^{\pm}) = 0.67$. The same result



is obtained from the slope of a plot of $\log k_1^{\text{OH}}$ vs. $\log (K_1^{\text{Pip}}K_a^{\pm})$ shown in Figure 9 for 50% Me₂SO. Note that in contrast to the Hammett plots, the 4-OMe and 4-NMe₂ points do not deviate from the line in Figure 9. This is because of a corresponding negative deviation of these points from the Hammett plot for $K_1^{\text{Pip}}K_a^{\pm}$.²⁶

In a first approximation, we may interpret these ρ_{nor} values to mean that rehybridization of the α -carbon (site of nucleophilic attack) and charge development on the C(CN)₂ moiety have made approximately 67% progress at the transition state. However, it is likely that ρ_{nor} actually overestimates the progress of these two processes because other factors tend to increase $\rho(k_1^{\text{OH}})$ and with it ρ_{nor} .

One such factor is that resonance stabilization of the carbanion is likely to lag behind charge development which places the developing negative charge closer to the aryl substituent in the transition state than in the product ion.⁴ Even though this kind of lag or "imbalance"²⁸ is typically much smaller with cyano-stabilized carbanions than with say nitro- or carbonyl-stabilized ones,⁴ it is probably not altogether negligible. A second factor which may increase $\rho(k_1^{\text{OH}})$ but not $\rho(K_1^{\text{OH}})$ or $\rho(K_1^{\text{Pip}}K_a^{\pm})$ is the electrostatic effect²⁹ of the residual negative charge on the attacking hydroxide ion in the transition state.

We thus conclude that ρ_{nor} gives an approximate upper limit of the progress of rehybridization and charge development on the C(CN)₂ moiety.³⁰

Solvent Effect on K_1^{OH} . For the unsubstituted BMN, we have estimates for K_1^{OH} in water and in 50%, 60%, and 70% Me₂SO

(26) Bernasconi, C. F.; Killion, R. B., unpublished results.

(27) Note that $\rho(K_1^{\text{Pip}})$ would not be a good approximation of $\rho(K_1^{\text{OH}})$ because K_1^{Pip} refers to the formation of a zwitterion, while $K_1^{\text{Pip}}K_a^{\pm}$ and K_1^{OH} refer to the formation of an anionic adduct.

(28) (a) Jencks, D. A.; Jencks, W. P. *J. Am. Chem. Soc.* **1977**, *99*, 7948.

(b) Sayer, J. M.; Jencks, W. P. *J. Am. Chem. Soc.* **1977**, *99*, 464.

(29) Young, P. R.; Jencks, W. P. *J. Am. Chem. Soc.* **1979**, *101*, 3288.

(30) We are implicitly assuming that rehybridization and charge development are synchronous. If there was an imbalance between these two processes, ρ_{nor} would be the upper limit of some weighted average in the progress of these two processes. For an example of an imbalance between changes in hybridization and other processes, see ref 28b.

(24) Yukawa, Y.; Tsuno, Y. *Bull. Chem. Soc. Jpn.* **1959**, *32*, 971.

(25) See, e.g.: Rappoport, Z.; Ladkani, D. *Chem. Scr.* **1974**, *5*, 124.

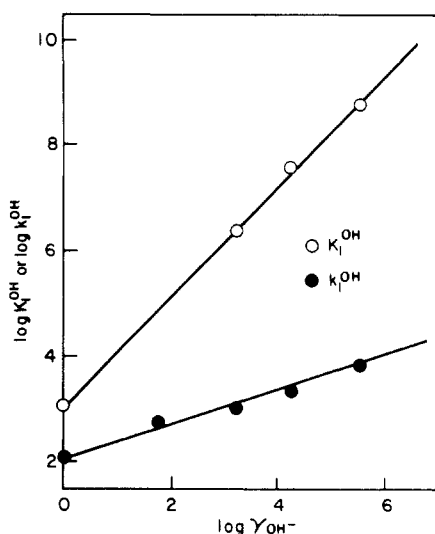


Figure 10. Plots of $\log K_1^{\text{OH}}$ and $\log k_1^{\text{OH}}$ for BMN vs. $\log \gamma_{\text{OH}^-}$.

(Table IV). K_1^{OH} is seen to increase strongly when Me_2SO is added to the solvent. For example, for the change from water to 70% Me_2SO , K_1^{OH} increases almost 5×10^5 -fold.

Solvent effects on equilibria are conveniently expressed in terms of the contribution by the solvent activity coefficient³¹ of each species involved in the equilibrium. Thus, for the solvent effect on K_1^{OH} , we may write eq 14. γ_{OH^-} , γ_{BMN} , and γ_{TOH^-} are the solvent activity coefficients for the transfer of OH^- , BMN, and TOH^- , respectively, from water to a Me_2SO -containing solvent.

$$\delta \log K_1^{\text{OH}} = \log \gamma_{\text{OH}^-} + \log \gamma_{\text{BMN}} - \log \gamma_{\text{TOH}^-} \quad (14)$$

A plot of $\log K_1^{\text{OH}}$ vs. $\log \gamma_{\text{OH}^-}$, with $\log \gamma_{\text{OH}^-}$ values taken from Wells³² and listed in Table VI, is shown in Figure 10. It reveals an excellent correlation with slope = 1.03 ± 0.02 (correlation coefficient 0.999). This indicates that the effects of $\log \gamma_{\text{BMN}}$ and $\log \gamma_{\text{TOH}^-}$ approximately cancel each other³³ (eq 14); i.e., the entire solvent effect on K_1^{OH} can be attributed to the reduced solvation of the hydroxide ion.

Solvent Effect on k_1^{OH} . The k_1^{OH} values increase significantly with added Me_2SO but the increase is not nearly as dramatic as for K_1^{OH} . For example, for the parent BMN, k_1^{OH} increases 54-fold from water to 70% Me_2SO , while K_1^{OH} increases 4.6×10^5 -fold for the same solvent change.

Since the increase in K_1^{OH} is satisfactorily correlated with γ_{OH^-} (Figure 10), one may expect the same to hold true for k_1^{OH} , as expressed in eq 15. A plot of $\log k_1^{\text{OH}}$ for BMN is included in Figure 10; it yields $\beta_{\text{nuc,sol}} = 0.30 \pm 0.02$ (correlation coefficient 0.995). The fact that the correlation of $\log k_1^{\text{OH}}$ with $\log \gamma_{\text{OH}^-}$

$$\delta \log k_1^{\text{OH}} \approx \beta_{\text{nuc,sol}} \log \gamma_{\text{OH}^-} \quad (15)$$

is not quite as good as that of $\log K_1^{\text{OH}}$ could indicate that here the $\log \gamma_{\text{BMN}}$ and/or $\log \gamma_{\text{TOH}^-}$ terms may not be canceling or be negligible. If, for example, k_1^{OH} was more sensitive to $\log \gamma_{\text{TOH}^-}$ than to $\log \gamma_{\text{OH}^-}$, a term in $\log \gamma_{\text{TOH}^-}$ as in eq 16 could become significant if $\alpha_{\text{nuc,sol}} \gg \beta_{\text{nuc,sol}}$ even though $\log \gamma_{\text{TOH}^-} \ll \log \gamma_{\text{OH}^-}$.

$$\delta \log k_1^{\text{OH}} \approx \beta_{\text{nuc,sol}} \log \gamma_{\text{OH}^-} - \alpha_{\text{nuc,sol}} \log \gamma_{\text{TOH}^-} \quad (16)$$

For the breakdown of T_0^- into $\text{PhCH}=\text{O}$ and $\text{CH}(\text{CN})_2^-$ (k_4 step in Scheme I), we have shown that the rate constant is indeed

more sensitive to the solvational changes in $\text{CH}(\text{CN})_2^-$ than to those in T_0^- .^{2b} This was expressed by an equation analogous to eq 16 (eq 17), with $\beta_{\text{N,sol}} \approx 0.57$ and $\beta_{\text{lg,sol}} \approx 0.78$.^{2b}

$$\delta \log k_4 \approx \beta_{\text{N,sol}} \log \gamma_{\text{T}_0^-} - \beta_{\text{lg,sol}} \log \gamma_{\text{CH}(\text{CN})_2^-} \quad (17)$$

We have not attempted to analyze the solvent effect on k_1^{OH} via eq 16. Not only is $\log \gamma_{\text{TOH}^-}$ more difficult to estimate than $\log \gamma_{\text{CH}(\text{CN})_2^-}$,^{2b} the absolute value of $\log \gamma_{\text{TOH}^-}$ is so much smaller than that of $\log \gamma_{\text{OH}^-}$ that a relatively small error in $\log \gamma_{\text{TOH}^-}$ would have such a large effect on the calculated $\alpha_{\text{nuc,sol}}$ values as to make the results meaningless.

The $\beta_{\text{nuc,sol}}$ value of ≈ 0.30 calculated from eq 15 may be regarded as an approximate measure of the degree of charge transfer from OH^- to the substrate in the transition state, and with it perhaps of the degree of C–O bond formation. It is interesting that this value is substantially lower than $\rho_{\text{nor}} = 0.67$. This inequality represents another example of an imbalance in structure reactivity parameters.

There are several factors which probably all contribute to this imbalance. Two of them were discussed before: they are the expected lag in the resonance stabilization of the adduct and the electrostatic effect of the residual negative charge on the attacking hydroxide ion. Both factors tend to enhance ρ_{nor} .

The third is desolvation of OH^- which is ahead of C–O bond formation. This is a rate-retarding effect in reactions of OH^- and other highly basic oxyanions which has been observed frequently.^{13,17,34,35} This effect is magnified upon addition of Me_2SO ,^{2b,36} which thus leads to a reduction in $\beta_{\text{nuc,sol}}$.

There is one factor which tends to counteract the observed imbalance by increasing $\beta_{\text{nuc,sol}}$. It is the accelerating effect on the intrinsic rate constant (and hence k_1^{OH}) of carbanion-forming reactions by added Me_2SO .^{17,36} This effect is likely to be small for a malononitrile-type anion, though, because $\log \gamma_{\text{TOH}^-}$ is probably very small.³⁷

Substituent Effect/Solvent Effect Cross Correlation. Plots of $\log k_1^{\text{OH}}$ vs. $\log \gamma_{\text{OH}^-}$ for the substituted BMNs are very similar to the one shown in Figure 10 for BMN. They afford the $\beta_{\text{nuc,sol}}$ values summarized in Table VI. The small substituent dependence of $\beta_{\text{nuc,sol}}$ has its counterpart in the small solvent dependence of the $\rho(k_1^{\text{OH}})$ values (Table VI). The interdependence of these two effects can be expressed by eq 18 which is another example of a cross-correlation coefficient.²⁸ In keeping with Jencks and Jencks,²⁸ we use the symbol p_{xs} where s stands for solvent. On the basis of BMN, BMN-Cl, and BMN- NO_2 , we obtain $\partial \rho(k_1^{\text{OH}})/\partial \log \gamma_{\text{OH}^-} = 0.047 \pm 0.029$ and $\partial \beta_{\text{nuc,sol}}/\partial \sigma = 0.027 \pm 0.018$ which are barely distinguishable from zero.

$$p_{\text{xs}} = \frac{\partial \rho(k_1^{\text{OH}})}{\partial \log \gamma_{\text{OH}^-}} = \frac{\partial \beta_{\text{nuc,sol}}}{\partial \sigma} \quad (18)$$

Experimental Section

Materials. The benzyldene malononitriles were available from previous studies.^{2b,11} Boric acid (Mallinckrodt, AR grade) and cacodylic acid (Sigma, AR grade) were used as such. The benzaldehydes (Aldrich) were purified according to literature procedures.³⁸ Piperidine was purified and stored as described before.³⁹ Reagent grade dimethyl sulfoxide (Mallinckrodt) was stored over 4-Å molecular sieves prior to use. All other chemicals used were of AR grade quality and used without further purification.

Reaction Solutions and pH Determinations. Solutions were prepared by adding appropriate amounts of aqueous stock solutions to a measured amount of Me_2SO in the case of 30% and 50% Me_2SO (v/v) of the final

(31) Parker, A. J. *Chem. Rev.* **1969**, *69*, 1.

(32) The values given in Table VII are interpolated from: Wells, C. F. In *Thermodynamic Behavior of Electrolytes in Mixed Solvents-II*; Furter, W. F., Ed.; Advances in Chemistry Series 177; American Chemical Society: Washington, DC, 1979; p 53.

(33) Neither $\log \gamma_{\text{BMN}}$ nor $\log \gamma_{\text{TOH}^-}$ is known, but their absolute values are expected to be much smaller than that of $\log \gamma_{\text{OH}^-}$. $\log \gamma_{\text{BMN}}$ must be small because it is uncharged,³¹ while $\log \gamma_{\text{TOH}^-}$ is probably smaller than the already small $\log \gamma_{\text{CH}(\text{CN})_2^-}$ for $\text{CH}(\text{CN})_2^-$ because the PhCHOH moiety is likely to reduce the solvation by water.

(34) (a) Hupe, D. J.; Wu, D. *J. Am. Chem. Soc.* **1977**, *99*, 7653. (b) Hupe, D. J.; Wu, D.; Shepperd, P. *J. Am. Chem. Soc.* **1977**, *99*, 7659.

(35) Jencks, W. P.; Brant, S. R.; Gandler, J. R.; Fendrich, G.; Nakamura, C. *J. Am. Chem. Soc.* **1982**, *104*, 7045.

(36) (a) Bernasconi, C. F.; Bunnell, R. D. *Isr. J. Chem.*, in press. (b) Bernasconi, C. F.; Paschalis, P. *J. Am. Chem. Soc.*, in press.

(37) For a thorough discussion of the connection between the solvent activity coefficient of a carbanion and the solvent effect on the intrinsic rate constant of its formation, see ref 17 and 36b.

(38) Perrin, D. D.; Armarego, W. L. F.; Perrin, D. R. *Purification of Laboratory Chemicals*, 2nd ed; Pergamon: New York, 1980; p 117.

(39) Bernasconi, C. F.; Carré, D. *J. Am. Chem. Soc.* **1979**, *101*, 2698.

solution volume. For higher Me₂SO proportions (60% and 70%), the reagents were taken first and the final volume was made up with Me₂SO. All pH measurements were performed on an Orion Research 611 digital pH meter (30% and 50% Me₂SO) and on a Metrohm/Brinkman 104 pH meter (60% and 70% Me₂SO). Both meters were equipped with a Corning No. 476022 glass electrode and a Beckman No. 39400 calomel reference electrode. The pH meters were calibrated for Me₂SO-water mixtures with buffers described by Hallé et al.⁴⁰

Kinetic Measurements. A Durrum-Gibson stopped-flow spectrophotometer with computerized data acquisition and analysis⁴¹ was used to monitor all the reactions except those involving the piperidinium ion catalysis. For this purpose, a Durrum multimixing system (Model D-

132) was used. In the first stage, T_{OH}⁻ was generated by mixing the substrate solution with 0.2 M KOH. The hydroxide ion concentration now was 0.1 M. In the second mixing, different amounts of a piperidine buffer were injected (which also contained HCl to neutralize the 0.1 M hydroxide remaining after the first mixing) after aging the first mixture for about 80 ms. This aging time assured that the formation of T_{OH}⁻ was complete.

Acknowledgment. This research was supported by Grants CHE-8024261 and CHE-8315374 from the National Science Foundation.

Supplementary Material Available: Tables of τ^{-1} values as functions of [KOH] and piperidinium ion concentration in water, Me₂SO solutions, and Me₂SO-water solutions at 20 °C (9 pages). Ordering information given on any current masthead page.

(40) Hallé, J.-C.; Gaboriaud, R.; Schaal, R. *Bull. Soc. Chim. Fr.* 1970, 2047.

(41) Developed by Dr. F. A. Brand.

Temperature-Dependent Stereoselectivity and Hydrogen Deuterium Kinetic Isotope Effect for γ -Hydrogen Transfer to 2-Hexyloxy Radical. The Transition State for the Barton Reaction

Mark M. Green,^{*1} Barbara A. Boyle,¹ M. Vairamani,¹ Triptikumar Mukhopadhyay,¹ William H. Saunders, Jr.,² Phillip Bowen,³ and Norman L. Allinger³

Contribution from the Departments of Chemistry, Polytechnic University, Brooklyn, New York 11201, University of Rochester, Rochester, New York 14627, and University of Georgia, Athens, Georgia 30602. Received September 3, 1985

Abstract: The diastereomers of 5-deuterio-2-hexanol, prepared stereospecifically from acetol and lactic acid by using fermentation procedures, have been subjected to the Barton reaction with Ag₂CO₃/Br₂ in pentane over the temperature range -8.65 to 30.05 °C. The derived 2,5-dimethyltetrahydrofuran deuterium incorporation yields both the C-5 diastereotopic hydrogen stereoselectivity and the isotope effect (k_H/k_D) for the intramolecular hydrogen-transfer step. The isotope effect is classically temperature dependent, 5.82 (± 0.07), 30.05; 6.01 (± 0.22), 20.55; 6.81 (± 0.17), 10.55; 6.90 (± 0.08), 1.65; 7.47 (± 0.49), -8.65 °C, while the stereoselectivity is small, 1.23 (1.65 °C), and temperature independent. Molecular mechanics calculations show that conformations with linear arrangements of C₅, H, and O show small steric energy differences between the diastereotopic hydrogens at C-5. Calculations of isotope effects and their temperature dependencies for model transition states match the experimental data for only C₅, H, and O angles greater than 150°. The Hofmann-Loeffler-Freitag reaction of the cation radical of 5-deuterio-2-aminohexane exhibits an isotope effect ($k_H/k_D = 1.20$) and stereoselectivity ($k_a/k_b = 1.54/1$), both at 25 °C, for the comparable γ -hydrogen-transfer step suggesting a more acute angle of transfer than for the alkoxy radical.

Intramolecular transfer of carbon bound hydrogen to a heteroatomic radical site defines a set of reactions of long use in synthesis.⁴ The fact that little more is known of the hydrogen transfer transition states than their characteristic occurrence via six-membered rings follows from the kinetic difficulty of isolating the hydrogen transfer, which is rapid^{5,6} and, therefore, not rate determining, from the various steps in the overall mechanistic picture.⁴

Early discussions of intramolecular hydrogen transfer noted the possible conflict between the expected propensity for a 180° C-H-X angle and more acute transfer angles which might minimize strain.⁷ It is known that the hydrogen selectivity of these reactions depends on the angle and distance between the transferred hydrogen and the abstracting atom and that these characteristics change with the state and identity of the abstracting radical.⁸⁻¹⁰ Attempts to understand the geometry of these intramolecular hydrogen-transfer reactions have centered on extrapolations from preferences in competitive transfers within a single molecule or observations that transfer does not occur. This

(1) Polytechnic University—address correspondence to M. M. Green.

(2) University of Rochester.

(3) University of Georgia.

(4) For an overview and leading references see: Carey, F. A.; Sundberg, R. J. *Advanced Organic Chemistry*, 2nd ed. Part A; Plenum Publishers: New York, 1984; pp 671-676.

(5) Beckwith, A. L. J.; Ingold, K. U. In *Rearrangements in Ground and Excited States*; DeMayo, P., Ed.; Academic Press: 1980; Vol 1, Essay 4, and particular p 251 ff.

(6) The rate constant for the oxygen radical system has been measured. See: Gilbert, B. C.; Holmes, R. G. G.; Laue, H. A. H.; Norman, R. O. C. *J. Chem. Soc., Perkin Trans. 2*, 1976, 1047.

(7) Corey, E. J.; Hertler, W. R. *J. Am. Chem. Soc.* 1960, 82, 1657. The expectation for linear transfer (see ref 5 above) is based on the linear transfer assumed for intermolecular SH₂ reactions at hydrogen and on the H₂ + H-reaction. See: Siegbahn, P.; Liu, B. *J. Chem. Phys.* 1978, 68, 2457. Truhlar, D. G.; Horowitz, C. J. *Ibid.* 1978, 68, 2466.

(8) Heusler, K.; Kalvoda, J. *Angew. Chem., Int. Ed. Engl.* 1964, 3, 525.

(9) Wolff, M. E. *Chem. Rev.* 1963, 63, 55.

(10) Carruthers, W. *Some Modern Methods of Organic Synthesis*; Cambridge University Press: London, 1971; Chapter 4.